minerals

MDPI

Article

Petrological, Geochemical, and Mineralogical Characterization of Three Coal Seams of the Imaloto Basin, Southwestern Madagascar

Moses Babila Ndasi [1,2], Nicola Jane Wagner [2,*] and Richard Viljoen [3]

[1] Luso Global Mining, Johannesburg 2092, South Africa
[2] DSI-NRF CIMERA, Department of Geology, University of Johannesburg, Johannesburg 2092, South Africa
[3] Bushveld Minerals, Sandton 2196, South Africa
* Correspondence: nwagner@uj.ac.za

Abstract: There is a lack of published literature on coal deposits in Madagascar. The Imaloto Basin is a sub-basin of the Morondava Basin, Southwestern Madagascar, and hosts the Sakoa Coal Measures. The aim of this study was to increase our understanding of the petrography, geochemistry, and mineralogy of coal deposits hosted in the Imaloto Basin. Three coal seams (from the bottom: Main Seam, Upper Seam, and Top Seam) were intersected during a drilling program conducted by the Lemur Holdings in 2019. Coal samples were characterized using organic petrography (type and rank determination); the ash chemistry was assessed (XRF), and the mineralogy was considered using X-ray diffraction. The depositional environment at the time of peat accumulation was considered. The Main Seam samples are of better quality compared to the Upper Seam and Top Seam samples in terms of calorific value (CV) and ash yield. The coals are borderline Sub-bituminous Low Rank A to Bituminous Medium Rank D. An abundance of inertinite macerals was determined in the Main Seam, while the Upper and Top Seams are more vitrinite-rich. An unusual mineral, possibly albite or analcime, was determined in samples with a high Na content. The Imaloto coal samples show varied depositional settings (dry forest swamp, wet forest swamp, and piedmont plain), which influences coal quality.

Keywords: Permian; Ecca; Karoo; inertinite; albite; facies

check for updates

Citation: Ndasi, M.B.; Wagner, N.J.; Viljoen, R. Petrological, Geochemical, and Mineralogical Characterization of Three Coal Seams of the Imaloto Basin, Southwestern Madagascar. *Minerals* **2024**, *14*, 620. https://doi.org/10.3390/min14060620

Academic Editors: Shifeng Dai and Davide Lenaz

Received: 14 April 2024
Revised: 31 May 2024
Accepted: 3 June 2024
Published: 18 June 2024

Copyright: © 2024 by the authors. Licensee MDPI, Basel, Switzerland. This article is an open access article distributed under the terms and conditions of the Creative Commons Attribution (CC BY) license (https://creativecommons.org/licenses/by/4.0/).

1. Introduction

Madagascar is the fourth largest island in the world with a population of 29.26 million [1]. It is one of the world's least developed countries, ranking 155 out of 187 on the Human Development Index [2]. In recent years, Madagascar's government has been working to expand its electricity supply and encouraging investment in the energy sector to stimulate the economy. But the ability to achieve this goal is constrained by challenges in the power sector and fuel supply. Madagascar's national electrification rate reached only 15% of the national need (53% in urban areas and 6.5% in rural areas) [3]. Although the country has the potential to generate 7800 MW of electric power from hydropower sources, only 2% of it is currently exploited [3]. Madagascar has 356 MW (hydro) and 150 MW (thermal) of installed generation capacity to serve a population of more than 29 million people. The average annual solar energy potential is estimated at 2000 kw/m^2, with additional potential for wind energy across multiple regions [3].

The government has made considerable efforts to promote the mining sector in general, but more particularly to encourage investments in the production of energy. The first discovery of coal in the Sakoa Basin, in the southwest of Madagascar, dates back to 1908. However, intensive exploration activities with objectives to develop industrial-scale mines has only taken place in the last two decades, initially by Pan African Mining Corporation (PAMC) from 2008 in the Sakoa Basin and in the Imaloto sub-basin by Lemur Holdings from

2009. Lemur Holdings is in the final phase of a Definitive Feasibility Study (DFS) to develop the Imaloto Coal Mine and a coal-powered fire station in Benenitra. It is anticipated that these investments will make a positive contribution to assisting Madagascar in resolving the energy shortfall.

The Sakoa Group hosts the coal-bearing formation in Madagascar, also known as the Coal Measures; this is considered to be equivalent to the Ecca Group of the Karoo Super Group [4]. The coalfields are located in the southernmost of three large sedimentary basins, namely, from the south: the Morondava Basin, the Mahajanga Basin, and the Diego Basin [4]. These basins developed prior to the separation of Madagascar from the east African mainland that occurred during the break-up of the Gondwana continent, about 180 Ma ago [4,5]. Continental break-up began with seafloor spreading between Africa and Madagascar in the Somali Basin after a brief phase of intra-continental rifting during the Jurassic magnetic quiet interval [6]. Madagascar, as part of Gondwana East (together with India, Australia, New Zealand, and Antarctica), drifted to the southeast in relation to Somalia along the trend of the Davie Ridge [7].

The Morondava Basin is the largest of the three basins and was the earliest to form. The Imaloto Basin is one of six separate elongated (NNW–SSE) sub-basins separated by faults that occur along the southern and southeastern margins of the Morondava Basin [5,8,9]. The Imaloto Basin is found some 20 km northeast of Benenitra, the main town under the jurisdiction of the Benenitra District in Madagascar.

Lemur Holdings Ltd. (LMR), a subsidiary of Bushveld Minerals, undertook substantial exploration drilling programs on its concessions in the Imaloto Basin. From February 2009 to December 2012, the company carried out a four-phased drilling program of 158 diamond drill holes giving a total of 19,572 m of core. These drilling programs led to the discovery of five coal seams in the basin, three of which were deemed to be economic, termed from the bottom: Main Seam, Upper Seam, and Top Seam. In 2019, the company drilled an additional eight diamond drill holes (total of 828.25 m of core), the focus of this study.

The 2019 drill holes supported a Social and Environmental Impact Assessment study (SEIA). Some holes were drilled to examine acid mine drainage from underground waters, while others were drilled for geotechnical studies. This also gave an opportunity to collect coal samples from the three economic coal seams for detailed petrographic (maceral type and rank), geochemical (ash chemistry), and mineralogical characterization (by X-ray diffraction) and to infer depositional environments at the time of seam formation. Twelve samples were collected from seven boreholes that intersected at least one of the three economic seams.

There is limited published information regarding coal quality, petrography, and geochemistry of coals from Madagascar. Gondwana coals (South Africa, South America, India, and Australia) are, as a generalization, of low quality, relatively challenging to beneficiate, and variable in rank (maturity) and organic matter composition compared to coals from other parts of the world [10–12]. It is envisaged that the findings of this study, though on a fairly limited number of samples, would provide reference information to mine engineers, metallurgists, and coal marketers for further development of the coals in Madagascar.

2. Geological Setting and Stratigraphy

The Morondava Basin was created by an early, failed rifting event that occurred in the Permo-Triassic period (the so-called Karoo Rift, 300–200 Ma) [8,9]. This event was characterized by extensive extensional faulting along a NNE–SSW axis, leading to a complex series of grabens, half-grabens, and horst blocks that make up the basin's eastern margin (Figure 1) [8,13]. Sediments deposited during this event were restricted to a narrow, NNW–SSE-oriented corridor some 90 km wide and over 500 km long (the "Karoo Corridor") that forms the eastern margin of the basin against a floor of Proterozoic crystalline basement rocks. Actual rifting occurred later and further to the west (c. 170 Ma), resulting in the unconformable deposition of Jurassic and Cretaceous sediments on top of the lower Karoo sediments in the Morondava Basin; and in the formation of the Mahajanga

and Diego (or Ambilobe) Basins further north [14]. All three basins extend offshore into the Mozambique Channel.

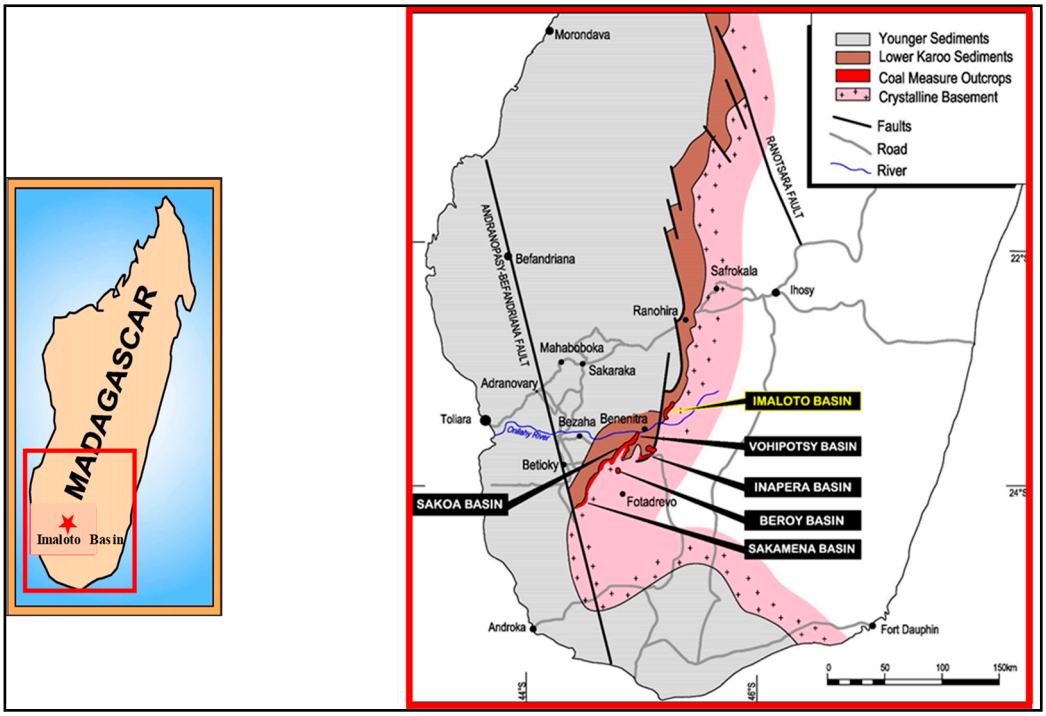

Figure 1. Location of the Imaloto Basin in the greater Morondava Basin [9].

Subordinate northeast–southwest faulting has also been reported by [14]. Faulting occurred contemporaneously with early sedimentation, resulting in individual fault-block basins (with downthrows mainly towards the west, or basin-wards) that developed local stratigraphic sequences which, while like those of adjacent blocks, are not easily correlatable [9]. The extensional strain imposed by incipient rifting resulted in the development of normal, steeply dipping fault planes [15]. The six sub-basins of the Morondava Basin (namely Sakamena Basin, Beroy Basin, Inapera Basin, Vohipotsy Basin, Sakoa Basin, and Imaloto Basin) are shown in Figure 1.

The Ecca Group (of the Karoo Super Group) is the predominant host of the coalfields of southern Africa [10,16]. The Karoo equivalent sediments in Madagascar are divided into three groups, known from bottom to top as the Sakoa, Sakamena, and Isalo Groups (Figure 2). In Madagascar, the Ecca Group is represented by the Sakoa Group, which constitutes the coal-bearing formation, also known as the Coal Measures [4]. The Sakoa Group is the oldest sedimentary unit in Madagascar, spanning the Late Carboniferous through Early Permian epochs [17] (Figure 2). It lies discordantly on the glacial series, equivalent to the Dwyka Tillite in South Africa, which in turn lies directly on the crystalline basement. The Sakoa Group is restricted to local, structurally confined basins [7,9]. Its total thickness varies dramatically from sub-basin to sub-basin, reaching up to 2000 m in the south and thinning gradually towards the northern Morondava Basin, where it eventually disappears under the Sakamena Group [4]. The difference in thickness from one sub-basin to another is related to the rifting event that occurred 170 Ma ago, resulting in individual fault-block basins that developed local stratigraphic sequences.

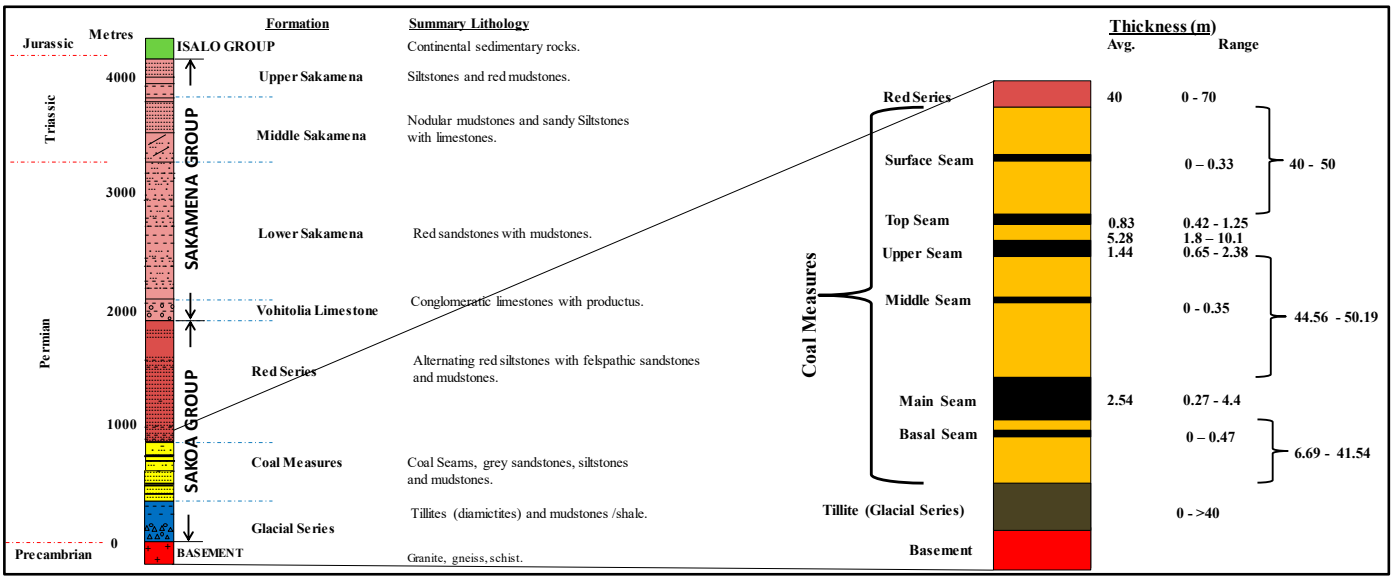

Figure 2. Generalized stratigraphic column of the Sakoa and Sakamena Groups, showing the position of the Imaloto Basin coal seams (diagram not to scale).

The Sakoa Group is exposed in the southern Morondava Basin and is predominantly a siliciclastic sequence comprising seven lithofacies associations, namely: diamictites; conglomeratic sandstones; sandstones; interbedded thin sandstones and mudstones; mudstones; coals and limestones [17]. These facies represent deposition in the extensional stages of continental rift development. The sediments were deposited predominantly on alluvial fans, and in braided to meandering stream and overbank environments [8]. Locally lacustrine and coal swamp environments formed in low areas of the basin floor during rift initiation, and subsidence rates remained constant throughout the Early Permian [9]. These were accompanied by a gradual reduction in relief of the basin margins and an increased geomorphic maturity of the fluvial systems flowing across the basin floor [9].

Towards the end of the Early Permian, the southern Morondava Basin was inundated by a marine transgression. This resulted in the deposition of the Vohitolia Limestone, which is underlain by the Red Series sandstones and mudstones [17]. Subsequent tectonic uplift and erosion resulted in a regional unconformity between the Sakoa Group and the overlying Sakamena Group, a thick sequence of tan-to-red sandstones and mudstones with occasional limestone units. The Sakamena Group is overlain by the Isalo Group, which consists of basal arkoses, reddish conglomerates and sandstones, overlain by fossiliferous calcareous sediments (white limestones, marls, oolitic limestones, etc.) typical of an Early-to-Middle Jurassic marine transgression.

The Sakoa coals are described by Besairie [5] as typical of Gondwana coals in terms of their physical characteristics and mode of occurrence. Coal deposits of the Sakoa Coalfields are similar to the multiple seam deposits of South Africa, such as the Witbank and Highveld [12], hosting several coal seams. According to Westcott and Diggens [17], the Sakoa coals were deposited as peats in a swampy environment. In areas where the coal seams outcrop, the coals are seen to be weathered and have acquired a flaky fragile texture.

At least five coal seams were identified in drill cores of historical drilling programs by Lemur Resources, namely, from top to bottom: Surface Seam (occasionally with a split), Top Seam, Upper Seam, Middle Seam, and Main Seam. The Main Seam is occasionally split at its base into a minor seam referred to as the Basal Seam when this is considerably thick enough (up to 0.45 m in some places). The relative positions of these coal seams, as well as the generalized stratigraphic column of the Sakoa and Sakamena Groups, are indicated in Figure 2.

3. Materials and Methods

Figure 3 shows a plan diagram of the spatial locations of LMR drill holes in the Imaloto Basin (2019 drill holes are labeled).

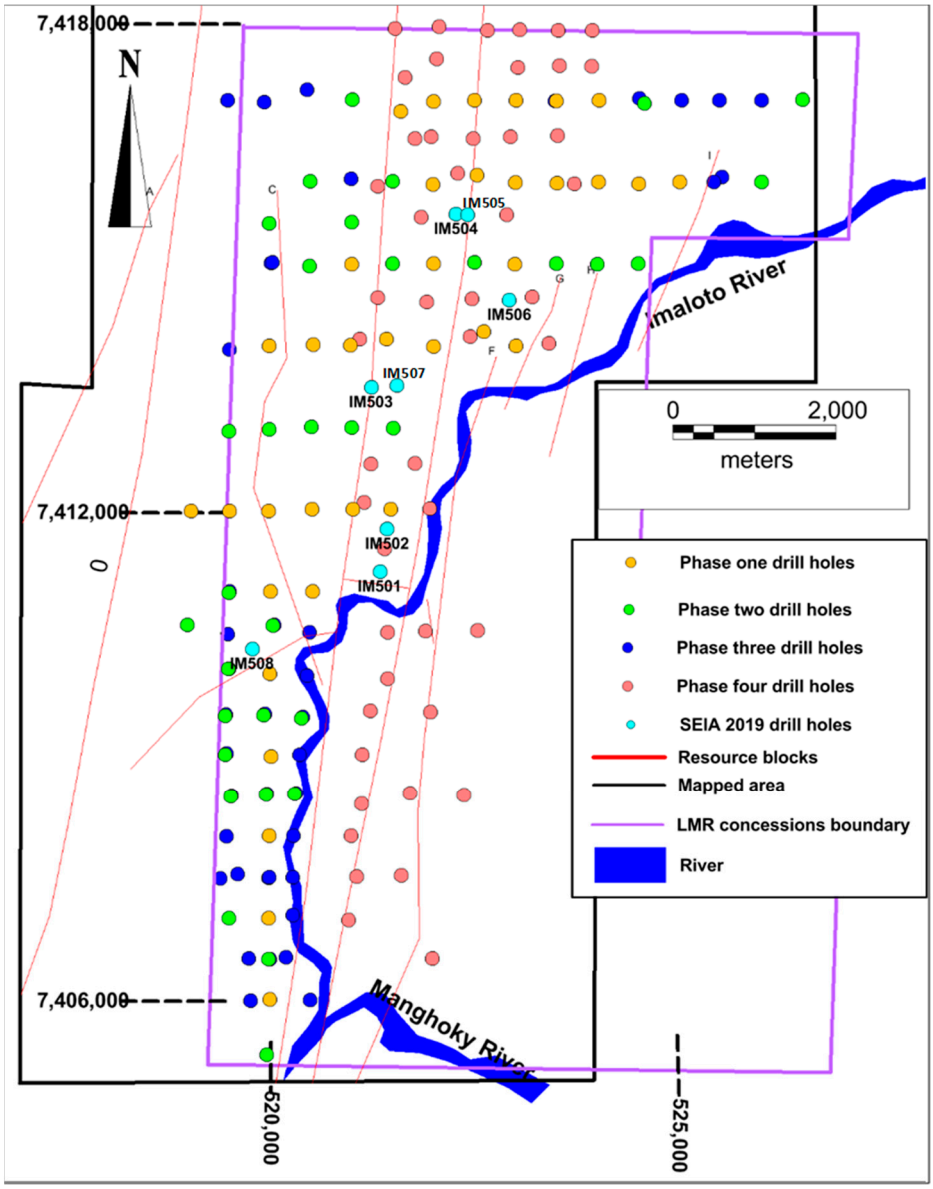

Figure 3. Plan diagram showing the location of the LMR drill holes in the Imaloto Basin. The 2019 drill holes are identified.

The cores from all LMR 2019 drill holes were logged, and whole core samples were collected in compliance with the SAMREC (2016) standards and stored in plastic sample bags under suitable conditions. Table 1 indicates the 12 samples collected from the 7 drill holes that intersected coal and their corresponding coal seams. The positions of the 2019 drill holes are shown in Figure 3. Unfortunately, not every coal seam was intersected in all the drill holes, impacting the number of samples available. Some seams pinch out towards the edge of the basin or against major faults, while others (particularly the Top Seam) are eroded in places. In drill hole IM503, for example, which is very close to IM507, only the Upper Seam was intersected. It is probable that the Main Seam in this hole pinched out against the fault, and the Top Seam eroded completely. The list of samples and thickness are listed in Table 1.

Table 1. List of coal samples from the LMR 2019 drilling program used in this study.

Hole ID	LMR Sample NO	UJ Sample ID	From (m)	To (m)	Thickness (m)	Date Sampled	COAL SEAM
IM503	SEIA01	2127	104.78	105.92	1.14	28/10/2019	Upper Seam
IM504	SEIA02	2128	90.82	91.56	0.74	29/10/2019	Top Seam
	SEIA03	2129	98.52	99.68	1.16	29/10/2019	Upper Seam
	SEIA04	2130	143.50	146.71	3.21	29/10/2019	Main Seam
IM505	SEIA05	2131	48.67	50.79	2.12	30/10/2019	Top Seam
	SEIA06	2132	97.20	100.50	3.30	30/10/2019	Main Seam
IM506	SEIA07	2133	26.74	27.82	1.08	10/11/2019	Top Seam
	SEIA08	2134	74.00	76.18	2.18	10/11/2019	Main Seam
IM507	SEIA09	2135	65.00	66.49	1.49	10/11/2019	Top Seam
	SEIA10	2136	115.59	117.92	2.33	10/11/2019	Main Seam
IM508	SEIA11	2137	23.81	24.86	1.05	10/11/2019	Main Seam
IM502	SEIA12	2138	37.49	39.11	1.62	10/11/2019	Upper Seam

The samples were submitted to the M & L Inspectorate (Bureau Veritas), Middelburg, South Africa, for coal quality analysis. M & L is a SANAS 17025 accredited independent coal laboratory. Sample preparation involved the crushing of the 12 coal samples to a top size of 15 mm. Each sample was homogenized and split into two halves. One half was bagged and stored, while the other half was milled further for the determination of ash, volatile matter, moisture, fixed carbon, gross calorific value (CV), and total sulfur (TS). Samples were analyzed using the lithium tetraborate fusion and acid dissolution method and read by XRF to determine the major elements and oxides.

Petrographic analyses were carried out at the Department of Geology, University of Johannesburg. Samples were crushed to between 2 and 5 mm using a mortar and pestle and then milled using a Retsch ZM200 mill, passing a −1 mm screen. The −30 µm particles were separated using a MACSALAB (ES200) electronic sieve shaker to obtain a −1 mm +30 µm size fraction for petrographic analysis. The petrographic blocks were prepared with a mixture of Epofix hardener and resin (diluted at a proportion of 1:7 mL) in a cup 3 mm in diameter and molded to make sample pellets. The pellets were placed in a Kulzer Technomat vacuum for 24 h to cure. Thereafter, the surface of each sample was ground and polished using a Struers Tegramin-20 polishing machine, to a final polish using a Struers type S oxide suspension. Sample preparation was carried out following the SANS/ISO [18] guidelines.

To determine the maceral composition (coal type) of the Imaloto coals, each polished pellet was analyzed using a Zeiss (Germany) Axio Imager (M2M) reflected-light petrographic microscope with a semi-automatic point-counting stage and Hilgers Fossil-Diskus retrofitted components and software (Fos 5.0.752#10670). Sample pellets were examined under an oil immersion lens at a total magnification of x500 using Zeiss Immersol oil (518 N), following [19]. At least 500 macerals and visible minerals were counted at traverses of 0.4 mm spacing and intervals of 0.5 mm between the traverse for each sample. For an appropriate distinction of the organic matter, sample blocks were examined under white-light mode and fluorescent mode. The terminology adopted by the International Committee for Organic Petrology (ICCP) was followed [19].

For the determination of coal rank by vitrinite reflectance, the Zeiss Axio Imager microscope with the Hilgers Diskus-Fossil system was calibrated using a Klein and Bekker YAG 0.900 standard following [20]. At least 100 reflectance measurements were taken on the polished and smooth surfaces of vitrinite particles, particularly on the homogeneous bands of collotelinite, under monochromatic non-polarized light. Random reflectance

measurements were recorded and reported with their standard deviations to three decimal places. Results were plotted on the coal classification scheme of the "Coal Classification of the Economic Commission for Europe [21]" to classify the samples.

Samples for XRD were crushed to −212 µm by XRD Analytical and Consulting in Pretoria. Diffractograms were obtained using a Malvern Panalytical Aeris diffractometer with PIXcel detector and fixed slits with Fe-filtered Co-Kα radiation. The phases were identified using X'Pert Highscore Plus 3.0. The analysis was both qualitative and quantitative, and the relative phase amounts (weight %) were estimated using the Rietveld method.

Scanning electron microscopy with energy-dispersive X-ray spectroscopy (SEM-EDX) was carried out at the University of Johannesburg Spectrum facility using a Tescan Vega to specifically understand the concentration and distribution of Na in coal sample 2131 (high $Na0_2$). The block mount used for petrography was repolished and carbon-coated.

4. Results

4.1. Coal Quality

Table 2 provides the data pertaining to the general qualities of the samples obtained from the three seams. The Main Seam includes fairly good-quality coal samples in terms of CV and ash yield but with slightly higher sulfur content than the Upper Seam and Top Seam samples. The average CV in the Main Seam is 22.8 MJ/Kg, 18.1 MJ/Kg in the Upper Seam, and 13.9 MJ/Kg in the Top Seam. The Main Seam average ash yield is 24.4% and ranges from 19.3% to 28.2%. Some samples in the Upper Seam (sample 2127 with 60.8% ash) and Top Seam (sample 2131 with 61.9% ash and sample 2135 with 61.2% ash) have ash values that fall out of the classification of coal (>50 wt% ash) and hence are referred to as carbonaceous shales, according to ISO [22]. The moisture content is similar in all three seams, but the average fixed carbon (FC) yield is higher in the Main Seam (43.8%) than in the Upper Seam (34%) and Top Seam (25%).

Table 2. General qualities of the 2019 Imaloto drilling program samples (air-dried).

Seam	Sample Number	Mass as Received	Moisture (Inherent)	Ash	Volatile Matter	Fixed Carbon	Total Sulfur	Gross CV
		(Kg)	%	%	%	%	%	MJ/Kg
Top Seam	2129	5.18	3.3	49.2	22.1	25.4	2.30	14.95
	2131	11.04	3.7	61.9	16.2	18.2	1.11	9.79
	2133	1.22	4.4	31.8	27.3	36.5	2.09	20.50
	2135	4.29	3.7	61.2	15.2	19.9	1.66	10.16
Top Seam Average			3.78	51.03	20.20	25.00	1.79	13.85
Upper Seam	2127	5.85	3.4	60.8	16.2	19.6	0.96	10.01
	2128	2.83	3.9	36.5	25.8	33.8	2.75	19.20
	2138	2.47	4.8	17.7	28.9	48.6	2.22	24.97
Upper Seam Average			4.03	38.33	23.63	34.00	1.98	18.06
Main Seam	2130	12.77	4.4	20.8	26.2	48.6	2.30	24.15
	2132	12.94	4.5	26.9	23.7	44.9	1.68	22.09
	2134	5.76	3.4	27.0	29.9	39.7	1.87	22.62
	2136	4.97	4.7	19.3	26.8	49.2	1.81	24.20
	2137	1.44	4.8	28.2	30.2	36.8	2.35	21.07
Main Seam Average			4.36	24.44	27.36	43.84	2.00	22.83
Overall Average			4.08	36.78	24.04	35.10	1.93	18.64

The Imaloto samples have a medium sulfur content. The overall average TS content is 1.9% and ranges from 1.7% to 2.4% in the Main Seam, 1% to 2.8% in the Upper Seam and 1.1% to 2.3% in the Top Seam. The medium sulfur content suggests a moderate input of sulfur-bearing water transgression during the peat and coal formation processes [23], assuming that the sulfur is of syngenetic origin.

The coal quality results obtained from the 2019 drilling program of the Imaloto Basin are comparable to those reported by [12] and others for South Africa, Botswana, and Mozambique coals. The results are very similar to those reported by [24] from historical drilling of 2009 to 2012 in the Imaloto Basin. The average volatile matter (VM) is 24%, which is very close to the 24.2% reported by [24]. Only the CV of the Upper Seam shows a significant deviation from the [24] results, with results of the 2019 drilling showing an overall average of 13.9 MJ/Kg, whereas [24] reports an overall average CV of 16.6 MJ/Kg.

4.2. Petrography

Petrographic assessment of the relative abundance and composition of the major maceral groups (vitrinite, inertinite, and liptinite) in the 12 coal samples analyzed shows that samples of the Main Seam have a higher abundance of inertinite macerals than vitrinite and liptinite macerals (Table 3, Summary Table). High inertinite content, especially inertodetrinite, is an indication of peat mires formed in fluctuating and low water table. The Upper Seam and Top Seam contain more vitrinite macerals compared to inertinite and liptinite maceral groups. Figure 4 is a clustered columnar plot of the relative abundance of the three maceral groups in the Main Seam, Upper Seam, and Top Seam. Photomicrographs of selected macerals identified in the analyzed coal samples are shown in Scheme 1a–l. The detailed petrographic data are shown in Table 3.

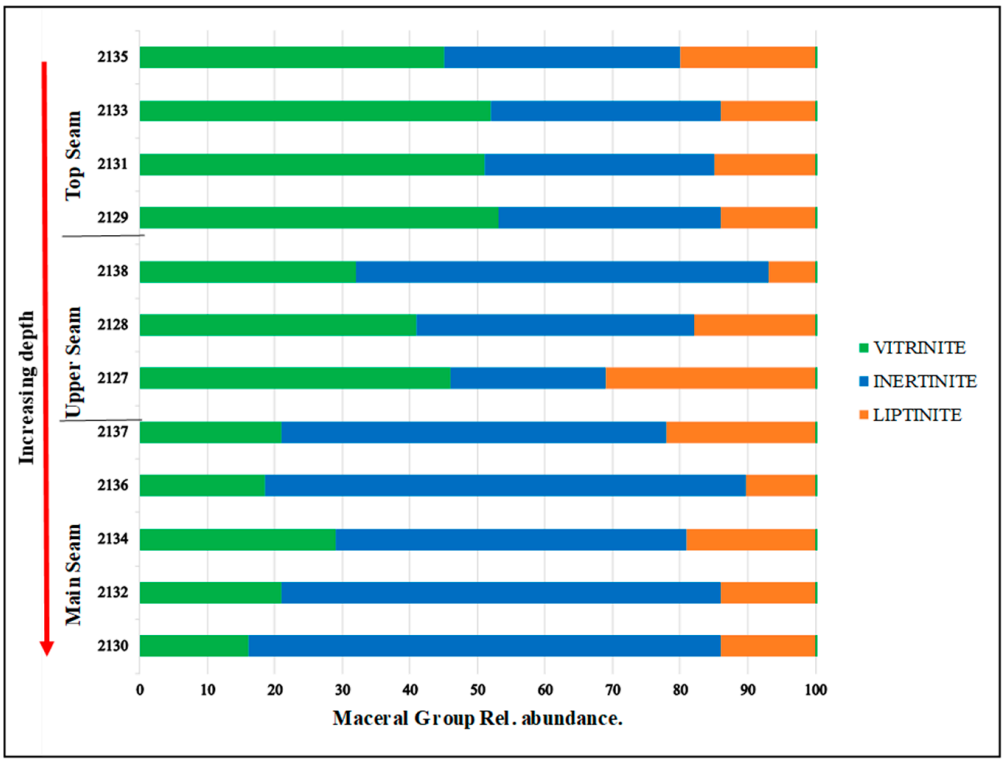

Figure 4. Relative abundance of the maceral groups in the Main Seam, Upper Seam, and Top Seam (vol.% mmf).

Table 3. Macerals and maceral groups' totals (vol.%) of the Main Seam, Upper Seam, and Top Seam of the Imaloto Basin samples. (Mineral matter: mmf = mineral matter free).

Coal Seam		Main Seam												Upper Seam						Top Seam					
UJ Sample ID		2130		2132		2134		2136		2137		2127		2128		2138		2129		2131		2133		2135	
	Maceral Vol. %	I. mm	Mmf	I. mm	Mmf	I. mm	mmf	I. mm	mmf	I. mm	mmf	I. mm	mmf	I. mm	mmf	I. mm	mmf	I. mm	mmf	I. mm	mmf	I. mm	mmf	I. mm	mmf
Vitrinite	Telinite	1.0	2.0	-	-	3.0	4.0	0.6	0.9	12.0	14.0	3.4	8.0	3.0	5.0	4.2	7.0	2.0	5.0	1.2	3.5	2.2	3.0	1.2	4.0
	Collotelinite	1.1	1.0	1.0	2.0	5.3	8.0	8.3	12.0	-	-	7.6	20.6	13.3	25.0	5.3	7.0	13.0	27.0	5.5	20.9	15.0	24.0	11.0	28.0
	Vitrotelinite	4.5	8.0	2.0	3.0	-	1.0	-	-	-	-	-	1.0	1.8	4.0	1.1	1.0	4.0	8.0	3.3	8.0	0.3	1.0	1.0	4.0
	Collodetrinite	3.1	5.0	1-	16.0	1-	15.0	2.5	3.7	6.0	7.0	6.0	16.4	4.4	7.0	10.1	16.0	6.0	13.0	5.5	17.6	15.0	23.0	2.6	9.0
	Corpogelinite	-	-	-	-	-	1.0	1.3	1.9	-	-	-	-	-	-	-	1.0	-	-	-	-	-	1.0	-	-
	Gelinite	-	-	-	-	-	-	-	-	-	-	-	-	-	-	-	-	-	-	-	-	-	-	-	-
Inertinite	Fusinite	2.8	5.0	1.0	2.0	1.1	2.0	12.8	18.5	6.0	7.0	2.0	4.0	6.0	12.0	1.0	1.0	3.0	6.0	1.0	3.0	2.5	4.0	2.0	5.0
	Semi-fusinite	29.8	48.0	24.0	39.0	24.6	36.0	26.8	36.9	29.0	36.0	7.2	18.0	15.0	28.0	31.3	44.0	12.0	26.0	8.7	28.0	13.9	22.0	11.0	29.0
	Micrinite	-	-	-	-	-	-	-	-	-	-	-	1.0	-	-	-	-	-	-	-	-	-	-	-	-
	Macrinite	-	-	0.8	-	0.8	1.0	-	-	-	-	-	-	-	-	-	-	-	-	-	-	-	-	-	-
	Secretinite	-	-	-	1.0	0.2	1.0	3.8	5.6	-	-	-	-	1.0	1.0	-	-	1.0	1.0	-	-	-	-	-	1.0
	Funginite	-	-	-	-	-	-	-	-	-	-	-	-	-	-	-	-	-	-	-	-	-	-	-	-
	Inertodetrinite	10.2	17.0	14.0	23.0	9.0	12.0	5.7	8.3	12.0	14.0	-	-	-	-	10.2	15.0	-	-	1.0	3.0	5.0	8.0	-	-
Liptinite	Sporinite	7.9	14.0	7.9	14.0	12.5	19.0	6.4	9.3	17.0	22.0	11.0	29.0	9.0	17.0	5.0	7.0	6.0	14.0	5.0	15.0	8.0	13.0	8.0	2-
	Cutinite	0.2	-	-	-	-	-	0.6	0.9	-	-	1.0	2.0	1.2	1.0	-	-	-	-	-	-	-	1.0	-	-
	Other liptinite	-	-	-	-	-	-	-	-	-	-	-	-	-	-	-	-	-	-	-	-	-	-	-	-
Mineral matter	Clay	9.1		8.5		12.1		13.4		12.2		38.2		25.6		7.2		27.5		40.8		12.4		34.8	
	Quartz	2.8		5.4		8.4		8.3		-		6.8		4.0		4.2		10.8		9.9		9.2		13.4	
	Pyrite	19.2		14.9		4.1		7.0		-		1.6		11.9		15.1		3.9		6.8		12.0		5.7	
	Carbonates	4.1		5.1		3.8		2.5		-		4.0		1.0		3.3		3 5.5		2.8		1.0		3.3	
	Other	4.0		6.2		5.0		-		6.4		11.0		3.2		4.4		3.8		6.6		4.0		6.0	
Summary table	Vitrinite	10.0	16.0	13.0	21.0	18.0	29.0	12.7	18.5	18.0	21.0	17.0	46.0	22.0	41.0	20.0	32.0	25.0	53.0	16.0	51.0	32.0	52.0	16.0	45.0
	Inertinite	43.0	70.0	39.0	65.0	36.0	52.0	49.1	71.3	47.0	57.0	9.0	23.0	22.0	41.0	42.0	61.0	16.0	33.0	11.0	34.0	22.0	34.0	13.0	35.0
	Liptinite	8.0	14.0	8.0	14.0	13.0	19.0	7.0	10.2	17.0	22.0	12.0	31.0	10.0	18.0	5.0	7.0	6.0	14.0	5.0	15.0	8.0	14.0	8.0	20.0
	Mineral Matter	39.0		40.0		33.0		31.2		18.0		62.0		46.0		33.0		53.0		68.0		38.0		63.0	
	Total Inertinite	43.0	70.0	39.0	65.0	36.0	52.0	49.1	71.3	47.0	57.0	9.0	23	22.0	41.0	42.0	61.0	16.0	33.0	11.0	34.0	22.0	34.0	13.0	35.0
	Total Reactive Macerals	18.0	30.0	21.0	35.0	31.0	48.0	26.7	38.9	35.0	43.0	29.0	77.0	32.0	59.0	25.0	39.0	31.0	6	21.0	66.0	40.0	66.0	24.0	65.0

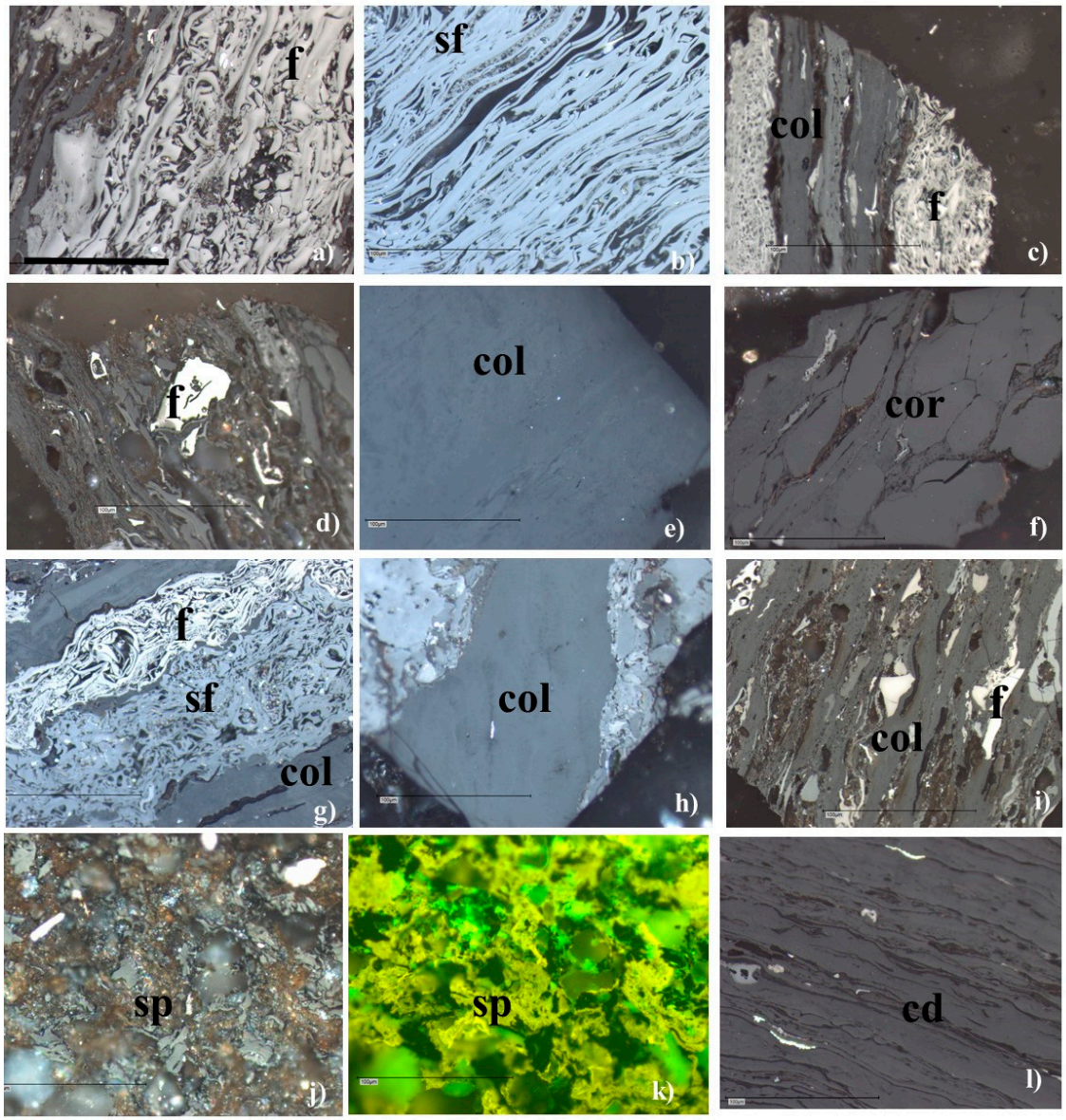

Scheme 1. Microphotographs depicting typically observed macerals in the Imaloto coal samples. (**a**) fusinite (f); (**b**) semi-fusinite (sf); (**c**) alternating bands of collotelinite (col) and fusinite; (**d**) fusinite fragments in a matrix of other macerals; (**e**) collotelinite; (**f**) corpogellinite (cor); (**g**) alternating bands of fusinite, semi-fusinite, and collotelinite; (**h**) collotelinite in inertinite macerals; (**i**) collotelinite alternating with bands of clay and inertinite fragments; (**j**) sporinite (sp) in a matrix of silicate minerals under incident white-light; (**k**) j under blue-light excitation; (**l**) collotelinite with cutinite (cd). (Images under oil immersion and total magnification ×500, scale bar is 100 µm, indicated in (**a**) and same for all images).

The average inertinite content (mmf) of the Main Seam is 63 vol.% (ranging from 52 to 71.3 vol.%), 41.7 vol.% for the Upper Seam (ranging from 23 to 61 vol.%), and 34 vol.% for the Top Seam (ranging from 33 to 35 vol.%). Semi-fusinite is the dominant inertinite maceral in all the coal seams, followed by inertodetrinite in the Main Seam and fusinite in the Upper and Top seams (Table 3). Macrinite and secretinite occur in very small proportions in all three seams. Fusinite was observed to occur in various modes, sometimes as fragments in a matrix of other macerals (Scheme 1d) or as alternating bands with other macerals (Scheme 1g).

In comparison, coals of the Highveld Coalfields of South Africa typically have high inertinite contents [25]. High inertinite contents have also been reported in coal seams of the Rukwa Basin in Tanzania and the Paraná Basin in Brazil [26], as well as in Zambian coals [25].

Vitrinite macerals are more abundant in the Upper Seam and Top Seam samples than in the Main Seam samples. The average vitrinite content (mmf) of the Main Seam is 21.1 vol.%, that of the Upper Seam is 39.7 vol.%, and that of the Top Seam is 50.3 vol.%. According to ISO/FDIS [22], the Main Seam and the Upper Seam can be classified as low vitrinite coals, while the Top Seam with an average vitrinite content of 50.3% (mmf) can be classified as medium vitrinite coal. Collotelinite is the vitrinite maceral with the highest abundance in the Upper Seam and Top Seam, while collodetrinite is more abundant in the Main Seam. Collotelinite is easily identified by the smooth surfaces, occurring sometimes as monomaceral (Scheme 1e), or as alternating bands with other macerals or sometimes alternating with clay minerals (Scheme 1i). Corpogellinite is rare and could be identified by the oval shape (Scheme 1f). No pseudovitrinite was observed.

A study by [27] on the petrography of the Songwe-Kiwira Coalfields of the Permian coal basins in Tanzania also found that seams developed in the lower parts of the basin have the lowest vitrinite contents. And, as is the case with the Imaloto Basin, seams that occur in the upper sections contain more vitrinite macerals. The Moatize coals of the Tete Province in Mozambique, which are thought to be of similar age (about 260 to 270 million years ago) and formed under similar climatic conditions in Gondwana, have very high vitrinite contents (above 80%) [28], indicating that the coals were developed in a wetter environment.

The average liptinite content (inc. mm) in the Main Seam is 10.3 vol.%, 8.3 vol.% for the Upper Seam, and 6.8 vol.% for the Top Seam. These proportions are comparable to those of South African coals, which generally have liptinite contents between 2 and 10 vol. % (inc. mm) [29,30]. Sporinite was observed under reflected light and confirmed under blue-light excitation (fluorescence mode) occurring most often in a matrix of silicate minerals (Scheme 1j,k). Minor cutinite was determined.

The petrographically observable minerals include clays and quartz (silicates), pyrite (sulfides), carbonates, and other minerals that could not be accurately classified. The relative abundance of these minerals in the three coal seams is presented in Table 3. Scheme 2a–h present photomicrographs of some minerals identified in the samples. Silicates (clays and quartz) were the most abundant minerals identified in these samples. The author in [31] also reported that clays are generally the most abundant minerals in coal, particularly in southern African coals. The abundance of clays in the samples range from 7 vol.% in the Upper Seam to 41 vol.% in the Top Seam. The clays identified in the Imaloto coals appear in bands alternating with various macerals (Scheme 2d), or as disseminated fine-grained mineral matter (probably syngenetic) or as small lenses, probably in-filling cell cavities, or replacing cell structures. The quartz grains were identified based on their glassy appearance (Scheme 2a–c); occasional colorful internal reflections were observed in the quartz grains, considered to be rutile rod inclusions.

The quartz content in these Imaloto samples is highest in the Top Seam and ranges from 9 to 13 vol.%. The average observable quartz content in the Main Seam is 5%, 5% in the Upper Seam, and 10.8% in the Top Seam. The quartz grains vary in shape, from sub-angular to sub-rounded, implying detrital origin.

Carbonate minerals can form by precipitation from the reaction of CO_2, H_2O, and calcium-rich components in the peat [32] or epigenetically through movement of groundwater fluids and hydrothermal activity [33,34]. The carbonate content is highest in the Main Seam, ranging from 2.5 to 5 vol.%, except for sample 2129 of the Upper Seam with a higher value of 6%. Calcite was identified as the most common carbonate mineral in the Imaloto coals, identified by a twinning and milky appearance, and confirmed by subsequent XRD and SEM analysis.

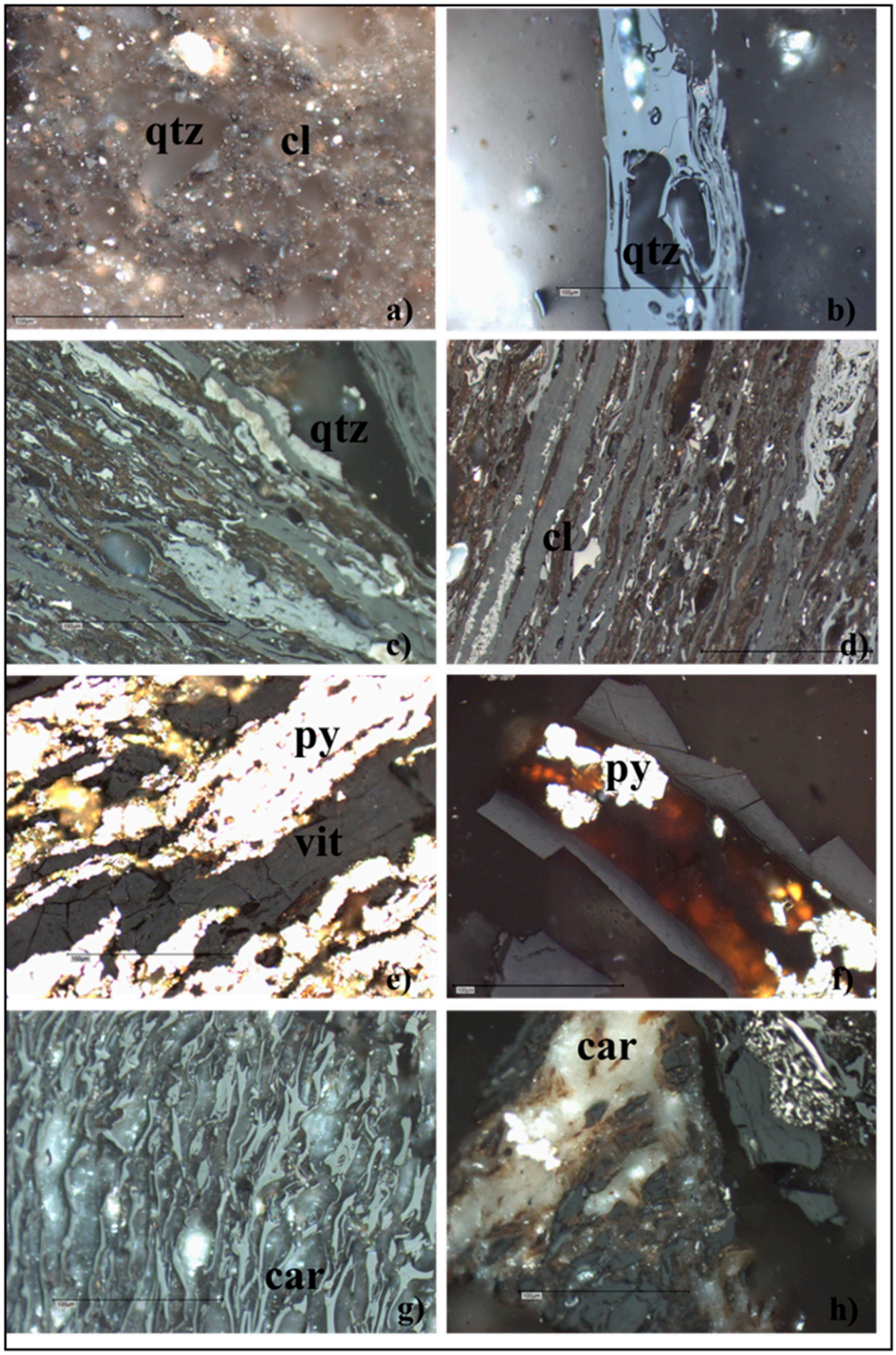

Scheme 2. Microphotographs of the mineral matter typically observed in the Imaloto coal samples: (**a**) silicates (clays (cl) and quartz (qtz)); (**b**) quartz grains engulfed in a fragment of semi-fusinite; (**c**) syngenetic quartz particle associated with macerals; (**d**) alternating bands of fine clays and macerals; (**e**) epigenetic pyrite (py) and vitrinite (vit); (**f**) pyrite concretions in liptinite; (**g**) carbonate (car) in-filling fusinite; (**h**) massive carbonate mineralization associated with vitrinite fragments and a pyrite grain. (Images under incident white light, under oil immersion and total magnification ×500, scale bar is 100 μm, indicated in image (**a**) and same for all images).

Pyrite is the most common sulfide mineral identified in the Imaloto samples. Under the microscope, in reflected light, pyrite grains were seen exhibiting a relief with extremely bright yellow colors. The pyrite minerals were mostly seen as large nodules concentrated into concretions, suggesting an epigenetic origin (Scheme 2e). The pyrite content distribution in the Imaloto coal seams is variable, ranging from 2 vol.% in the Upper Seam to an elevated value of 19 vol.% in sample 2130 of the Main Seam. The average pyrite content is 9% in the Main Seam, 9.5% in the Upper Seam, and 7.1% in the Top Seam. In general, there is a relationship between the pyrite and the TS content in the samples, whereby samples with higher pyrite contents tend to have a higher TS content. For example, sample 2130 of the Main Seam with a pyrite content of 19.2% also has a high TS content of 2.3%, sample 2138 of the Upper Seam with a pyrite content of 15.1% has a high TS content of 2.2%, while sample 2127 of the Upper Seam with a pyrite content of 1.6% only has a TS content of 0.9%.

The mean random reflectance values (%Vmr) were plotted on the Classification of Coals scheme of ISO/FDIS [22] to determine the rank of the coal samples (Figure 5). The plots show that the Imaloto samples fall between Sub-Bituminous Low Rank A to Bituminous Medium Rank D. The average %Vmr across the basin is 0.49%, placing the Imaloto coals, on average, in the Sub-Bituminous Low Rank A classification. Previous studies (e.g., [5]) have also described the Imaloto coals as sub-bituminous. Most of the Main Seam samples fall in the Bituminous Medium Rank D, with an average mean random reflectance value of 0.51%Vmr and ranging from 0.49% to 0.54%. Upper Seam samples are Sub-Bituminous Low Rank A, except for sample 2138, which is borderline Bituminous Medium Rank D. The average %Vmr of the Upper Seam is 0.48%, and 0.49% in the Top Seam.

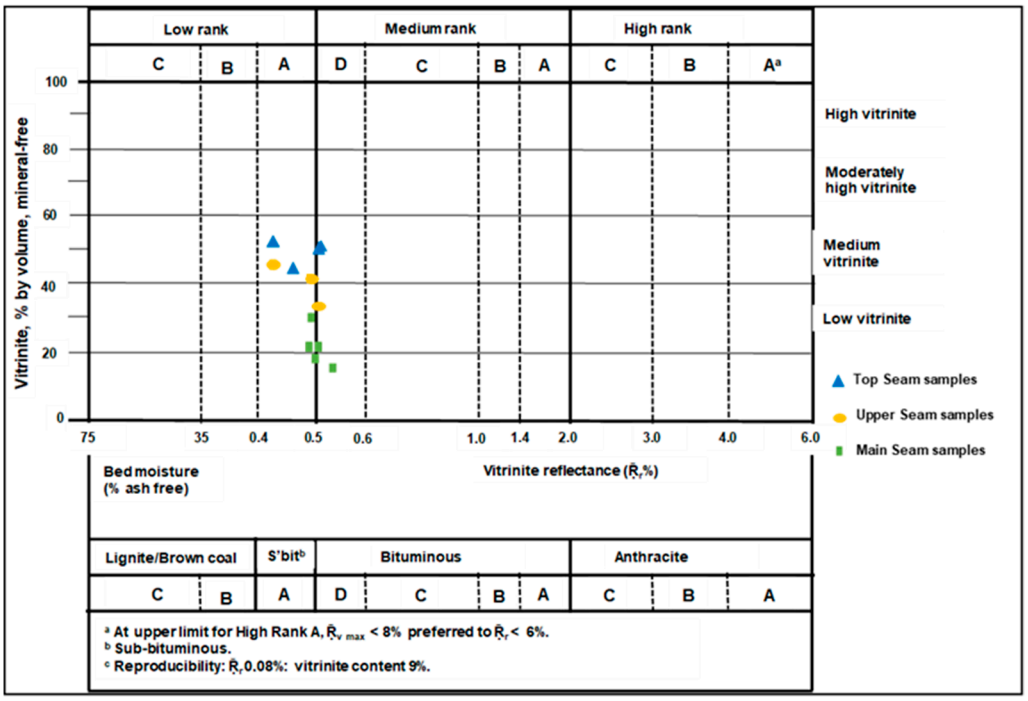

Figure 5. Plot of the Imaloto coals on the Classification of Coals scheme of ISO/FDIS [22].

There appears to be a trend of decreasing rank towards the surface. Samples from the deeper parts of the basin, especially the Main Seam, have higher reflectance values. No evidence of large igneous masses in the Imaloto Basin was found from the drill cores of the drilling programs of Lemur Holdings, nor in the literature review. This means, therefore, that the coal seams experienced the normal gradual metamorphism that occurs in response to rising temperatures and pressures with burial, which turns the initial peatland into progressively higher coal ranks during the coalification process [29].

4.3. Ash Chemistry and Mineralogy

The XRF data are presented in Table 4. SiO_2 is the oxide with the highest relative abundance in all the Imaloto samples, followed by Al_2O_3. There is an upward increase in the average relative abundance of SiO_2. The average SiO_2 content in the Main Seam is 48% (ranging from 31.1% to 56.1%), in the Upper Seam is 57.5% (ranging from 47% to 65.5%), and in the Top Seam is 58.6% (ranging from 54.1% to 59.3%).

Table 4. Chemical composition of the Imaloto coal ash (% air dry basis).

	Sample ID	SiO_2	Al_2O_3	Fe(tot)	Fe_2O_3	TiO_2	CaO	MgO	Na_2O	K_2O	MnO	P_2O_3	BaO	Cr_2O_3	Cu	Ni	SrO	V	Zn	ZrO_3	SO_3
Top Seam	2129	58.4	19.2	2.88	4.11	1.13	4.40	1.50	2.91	4.40	0.06	0.07	0.06	0.03	0.01	0.01	0.03	0.02	0.01	0.05	3.75
	2131	54.1	20.8	2.36	3.38	1.15	3.52	1.04	8.85	3.65	0.05	0.07	0.10	0.03	0.01	0.01	0.05	0.02	0.01	0.05	3.42
	2133	62.5	19.6	4.04	5.78	1.17	2.40	1.69	1.91	3.81	0.04	0.06	0.05	0.04	0.01	0.01	0.04	0.04	0.01	0.06	0.17
	2135	59.3	18.4	3.50	5.01	1.11	2.42	1.28	5.58	4.23	0.03	0.04	0.07	0.02	0.01	0.01	0.03	0.03	0.01	0.04	2.16
	Avg.	58.58	19.50	3.20	4.57	1.14	3.19	1.38	4.81	4.02	0.05	0.06	0.07	0.03	0.01	0.01	0.04	0.03	0.01	0.05	2.38
Upper Seam	2127	65.5	22.4	2.52	3.60	1.24	0.69	1.28	0.46	4.02	0.02	0.05	0.07	0.02	0.01	0.01	0.02	0.02	0.01	0.05	0.22
	2128	60.1	21.0	6.28	8.98	1.24	1.43	1.44	0.74	4.25	0.03	0.07	0.06	0.03	0.01	0.01	0.04	0.04	0.02	0.08	0.88
	2138	47.0	19.1	4.67	6.68	1.28	11.11	1.01	2.31	0.69	0.14	0.05	0.03	0.05	0.01	0.02	0.07	0.03	0.01	0.06	10.44
	Avg.	57.53	20.83	4.49	6.42	1.25	4.41	1.24	1.17	2.99	0.06	0.06	0.05	0.03	0.01	0.01	0.04	0.03	0.01	0.06	3.85
Main Seam	2130	50.4	19.1	4.70	6.72	1.59	9.04	0.94	2.90	0.59	0.10	0.06	0.02	0.03	0.01	0.01	0.07	0.01	0.01	0.05	8.69
	2132	56.1	20.0	5.28	7.55	1.95	3.37	0.80	6.76	1.01	0.06	0.09	0.04	0.04	0.02	0.01	0.04	0.02	0.00	0.07	2.72
	2134	55.8	20.6	3.84	5.49	1.84	5.52	1.20	3.63	1.03	0.04	0.04	0.03	0.04	0.02	0.01	0.12	0.02	0.00	006	4.79
	2136	47.3	19.9	3.75	5.37	1.75	11.07	0.87	2.33	0.73	0.12	0.06	0.03	0.04	0.01	0.02	0.07	0.02	0.00	0.06	10.79
	2137	31.1	11.9	3.88	5.56	0.82	28.60	0.90	5.97	0.26	0.26	0.14	0.01	0.05	0.01	0.01	0.09	0.02	0.00	0.04	14.78
	Avg.	48.14	18.30	4.29	6.14	1.59	11.52	0.94	4.32	0.72	0.12	0.08	0.03	0.04	0.01	0.01	0.08	0.02	0.00	1.24	8.35
Overall Average		54.0	19.3	4.0	5.7	1.4	7.0	1.2	3.7	2.4	0.1	0.1	0.0	0.0	0.0	0.0	0.1	0.0	0.0	0.1	5.2

Other common oxides are Fe_2O_3, CaO, K_2O, and SO_3, in amounts comparable to those found in most South African coals [35]. Na_2O was determined to be high in some samples, for example, 2131, 2132, and 2137, with a maximum value of 8.85% (see below for further discussion). Oxides like BaO, Cr_2O_3, and trace elements like Cu, Ni, V, and Zn occur in very small amounts.

The most common carbonate minerals in coals are calcite and dolomite, but also fluorapatite and ankerite [29,30]. The occurrence of these minerals in coals is indicated by the presence of CaO and MgO, which are present in significant amounts in the Imaloto coal samples (Table 4).

The diffractograms generated from the XRD analysis of the Imaloto samples are presented in Figure 6. The minerals determined are presented in Table 5. The clay minerals (illite, kaolinite, and smectite) dominate, with an overall average weight of 15%, and support the petrographic findings. Quartz is also prevalent, with an overall average of 8.5 wt %, and again supporting the petrographic findings The overall average weight % of pyrite is 1.7%, a trend comparable to the TS values (average 1.9%) reported in Table 2.

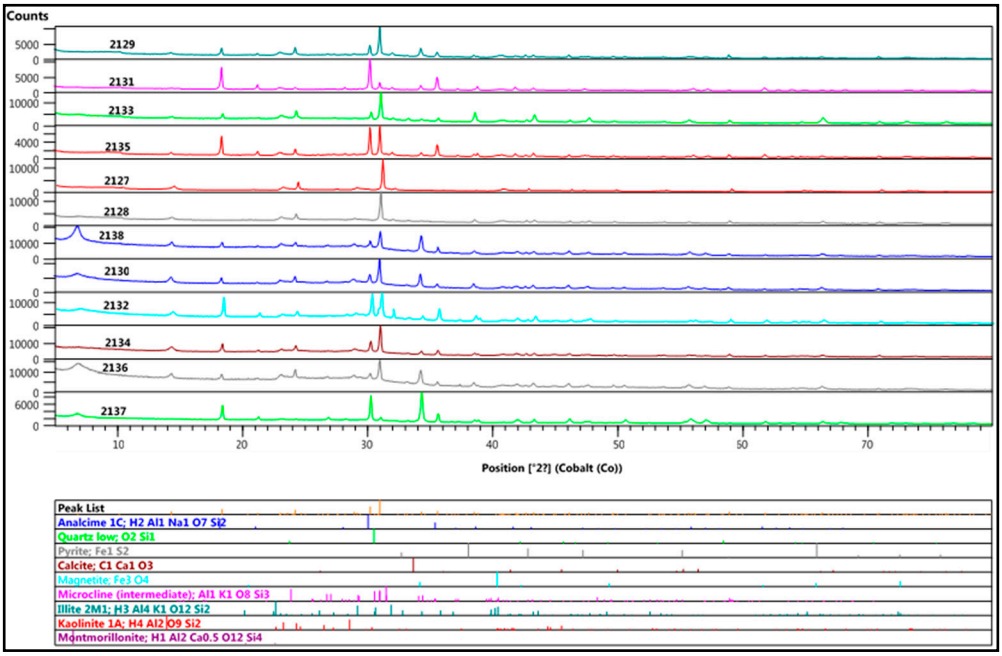

Figure 6. XRD spectra indicating mineral composition determined in the Imaloto samples (Main Seam = 2130, 2132, 2134, 2136, and 2137; Upper Seam = 2127, 2128, 2138, and 2129; Top Seam = 2131, 2133, and 2135).

Table 5. Mineral composition of Imaloto samples determined by XRD (weight %).

SEAM	Sample ID	Analcime	Quartz	Pyrite	Calcite	Magnetite	Microcline	Illite (I)	Kaolinite (K)	Smectite (S)	Total Clay (I + K + S)	Organic Matter
Top Seam	2129	8.6	13.1	1.5	3.6	0.4	3.3	8.3	6	4.9	19.2	50.3
	2131	44.2	4.8	0.8	2.8	0.4	3.5	6.9	1.4	3.7	12	31.4
	2133	4.6	9.2	5.1	0.4	0.2	2.1	4.9	4.7	5.9	15.5	63
	2135	25.1	13	1.9	1.4	0.5	4.6	8.1	3.7	6	17.8	35.6
	Avg.	20.6	10.0	2.3	2.1	0.4	3.4	7.1	4.0	5.1	16.2	45.1
Upper Seam	2127	0	21.2	0.5	0	0.4	4.4	10.6	13.1	13.6	37.3	36.3
	2128	0.1	12.9	2.4	0.1	0.2	2	5.6	9.2	6.2	21	61.2
	2138	2.3	3.5	0.9	3.1	0	0.4	0.6	4.4	4.9	9.9	79.7
	Avg.	0.8	12.5	1.3	1.1	0.2	2.3	5.6	8.9	8.2	22.7	59.1
Main Seam	2130	3	5.4	1.4	2.5	0	0.1	0.5	6.5	4	11.0	76.5
	2132	9.9	6.2	1.9	0.7	0	0.9	0	5.2	2.8	8.0	72.4
	2134	6.1	7.8	1.0	0.8	0	0	1.0	8.8	2.8	12.6	71.6
	2136	1.6	3.3	1.1	2.3	0	0.3	0.9	5.4	5.6	11.9	79.4
	2137	13.4	12.0	1.9	11.5	0.1	0	0	0.7	2.3	3.0	69.0
	Avg.	6.8	6.9	1.5	3.6	0.0	0.3	0.5	5.3	3.5	9.3	73.8
Overall Average		9.9	8.5	1.7	2.4	0.2	1.8	4.0	5.8	5.2	15.0	60.5

Mineral identification is largely based on peak shapes and position. Smectite, serpentine, vermiculite, chlorite, and kaolinite peaks were found to overlap, and further analysis may be necessary to clearly distinguish between these minerals. For example, smectite has a peak at 14 Angstrom, kaolinite and serpentine at 7, chlorite at 14 and 7.

Of particular interest is the determination of the mineral analcime (or analcite) in these samples, occurring in all three seams (Table 5), with an overall average composition across the seven drill holes of 9.9 wt.%. The abundance of analcime is highest in the Top Seam samples with an average of 20.6%, ranging from 4.6% in sample 2133 to 44.2% in sample 2131. Sample 2131, with the highest composition of analcime, also has the highest

composition of Na_2O (8.85%) (Table 4). Typically, Na_2O values for South African coals are below 1% [35].

Analcime (or analcite), with a chemical formula of $NaAlSi_2O_6 \cdot H_2O$, is a gray, white or colorless tectosilicate of the Zeolite Group [36]. It occurs in the vesicles or groundmasses of silica-poor mafic and intermediate igneous rocks such as basalts and phonolites, formed from late-stage hydrothermal solutions, or disseminated because of deuteric alteration. Analcime occurs in lake beds as a product of alteration from pyroclasts or clays or as a primary precipitate and can enter coal seams through percolating waters. It is authigenic in sandstones and siltstones [36]. The Precambrian Basement rocks of the Imaloto Basin are composed mainly of gneiss, migmatites, and pink granitic quartzites, which occur mostly on the eastern edge of the basin [13]. Medium-to-coarse-grained granites also occur in the southwestern edge of the basin, while occasional medium-grained dolerite dykes and fine-grained pale-to-grey lamprophyres also occur at different areas of the central and northern portions of the basin. It is probable that these rocks constitute the source rocks of the analcime in the Imaloto coals. However, further investigation is required.

As SEM-EDX cannot detect hydrogen (up to 1% in analcime), and because it is not always possible to obtain accurate oxygen values using EDX, the mineral was reported as albite (Figure 7). Another school of thought suggests that the reported grains in Figure 7 are detritic feldspar grains, which are altered within palaeomires or during transportation. Plagioclase (Na-bearing albite) is the primary source of sodium in coal. These minerals, however, were not observed in the SEM images. It is interesting to note that the EDX data indicate that Na is primarily linked to organic matter. The unusually high Na concentration in the organic matter may be the result of Na being released from albitophyre during weathering. It is probable that ground water carried the Na from the strata above and below into the coal, where it combined with organic matter, causing an enrichment of the coal in Na, and resulting in unusually high Na content.

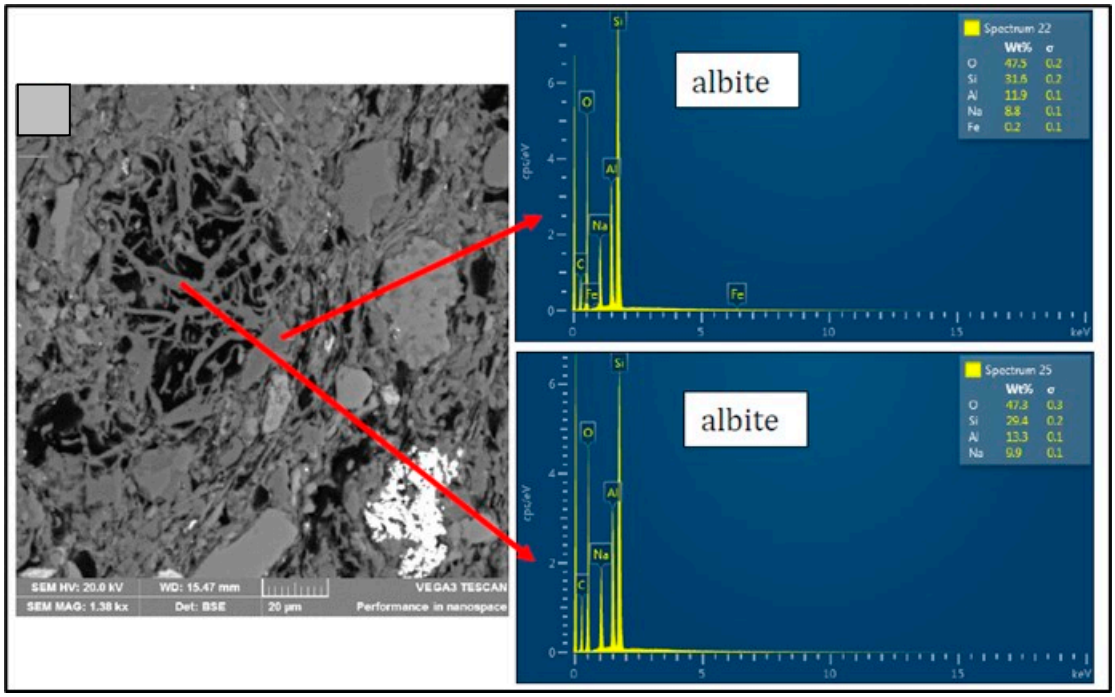

Figure 7. A SEM image and spectra of sample 2131 of the Top Seam, indicating albite.

Considering the inconclusive findings, this study concluded that the unusual mineral is analcime based on the XRD data, with Na also occurring in the organic matter. A further study may be required for further clarity on this unexpected finding. The occurrence of analcime is not noted in the literature on southern or east African coals. The authors in [37]

note the need to further investigate the source of Na (amongst other non-mineral elements) in coals.

5. Discussion

The Main Seam, which is the thickest seam at the bottom of the profile in the Imaloto Basin, presents better coal quality in terms of CV, ash yield, and FC content than the Upper Seam and Top Seam, which are located closer to the surface. The Main Seam, therefore, developed in an environment with abundant organic matter supply and a lower terrestrial source debris supply, as indicated by the lower ash. The difference in the clay contents of the three seams reflects the variation in the palaeo-depositional environments. It appears that the peat mire that formed the Upper Seam and Top Seam contained more terrestrial sediments that favored the decomposition of feldspar minerals into kaolinite. A ternary plot of the relative abundance of the maceral groups (vitrinite, inertinite, and liptinite) of the Imaloto coals is presented in Figure 8. The ternary plot was developed by [38] to show a scheme of depositional environments of coal formation using microlithotypes determined in Australian coals. In the current study, microlithotype analysis was not conducted, and hence the maceral groups were used to broadly infer the depositional environments of the Imaloto coals, as used by [39].

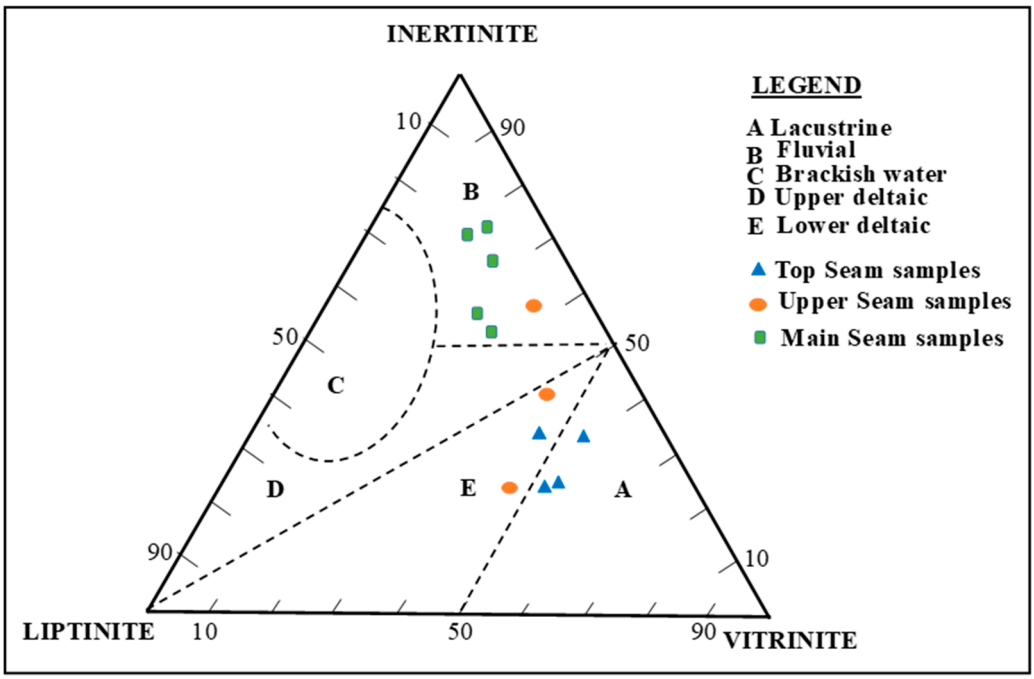

Figure 8. Ternary diagram used to indicate the depositional environments at the time of deposition for the three coal seams using maceral groups. (Modified from [38]) (Vol.% mmf).

Figure 8 shows that the Main Seam samples fall in the fluvial depositional environment, related to the high abundance of inertinite macerals in these samples. It is likely that the Main Seam was formed from highly altered and strongly degraded plant material, in an environment with fluctuating water table during peatification. High inertinite content is an indication of peat mires formed in fluctuating and low water tables. It also indicates that the main activity during this time was the circulation of water and re-deposition of peatified material.

Samples of the Upper Seam and Top Seam are more vitrinite-rich and fall largely in the lower deltaic and lacustrine depositional environments (Figure 8). Vitrinite macerals, particularly collotelinite, which is the dominant vitrinite maceral in the Imaloto coals, formed from lignin and cellulose of cell wall materials of woody plant tissues such as roots, leaves, branches, and trunks, as well as colloidal humic gels in the peatlands that were

rapidly covered by sediments or water, preventing them from severe biochemical alteration through oxidation [40]. It can therefore be postulated that the Upper Seam and Top Seam were formed in the waterlogged and relatively more anaerobic low areas of the basin floor during rift initiation, where subsidence rates remained constant throughout the Early Permian. Most often, the original cellular and woody parent materials that formed the vitrinite macerals are the same materials from which the inertinite macerals were derived in coals of the same rank [41].

Many other models have been used in analyzing coal facies such as the gelification index (GI), tissue preservation index (TPI), ground water index (GWI and variations), and vegetation index (VI), [39,42–45], which are based on quantitative amounts of coal constituents including macerals, microlithotypes, and minerals to determine palaeoenvironments. To consider the depositional environments of the Imaloto basin, the TPI and GI models of [43] were used as stated in the equations (Equations (1) and (2)) below:

$$\text{TPI} = \frac{\text{telinite} + \text{collinite} + \text{semi-fusinite} + \text{fusinite}}{\text{Detrovitrinite} + \text{macrinite} + \text{inertodetrinite}} \quad (1)$$

$$\text{GI} = \frac{\text{vitrinite} + \text{macrinite}}{\text{Semi-fusinite} + \text{fusinite} + \text{inertodetrinite}} \quad (2)$$

The TPI and GI values are presented in Table 6, while the plot is shown in Figure 9. The TPI values are generally high, and some samples (e.g., sample 2136 of the Main Seam, samples 2127 and 2128 of the Upper Seam, and samples 2129 and 2135 of the Top Seam) have very high TPI values that plot out the diagram. It seems therefore that this model is not suitable for all the samples. Other scholars (e.g., [39,43–45]) have discussed the shortcomings of facies models to determine depositional environments and have noted that these models are not applicable to all coals globally.

Table 6. TPI and GI values of the Imaloto coal samples.

Seam	Sample ID	TPI	GI
Top Seam	2129	3.0	1.7
	2131	1.9	1.5
	2133	1.7	1.5
	2135	5.1	1.3
Upper Seam	2127	2.9	2.1
	2128	6.4	1.0
	2138	1.8	0.5
Main Seam	2130	1.9	0.2
	2132	1.0	0.3
	2134	1.7	0.6
	2136	5.9	0.3
	2137	2.7	0.4

The samples with very high TPI values also have high fusinite contents (Table 3). The high TPI values of the Imaloto samples indicate that the plant material in the original mire was well preserved. Samples of the Upper Seam and Top Seam have high GI values. Teichmüller [40] noted that low GI and low TPI indices are indicative of dry circumstances, and high GI and high TPI indices are often indicative of wet conditions of peat formation. Samples of the Main Seam fall in the dry forest swamp and piedmont plain environments (Figure 9). Samples 2131 and 2133 of the Top Seam fall in the wet forest swamp environment. Only sample 2138 of the Upper Seam plots in the piedmont plain depositional environment.

The Imaloto samples show varied depositional settings (dry forest swamp, wet forest swamp, and piedmont plain), which influenced the maceral distribution, as seen in Figure 9. It should be noted that concerns regarding the use of the GI and TPI indices and depositional models based on maceral composition alone are well cited [45]. All properties must be considered, and the overprint of coalification and subsequent epigenetic impact must be considered.

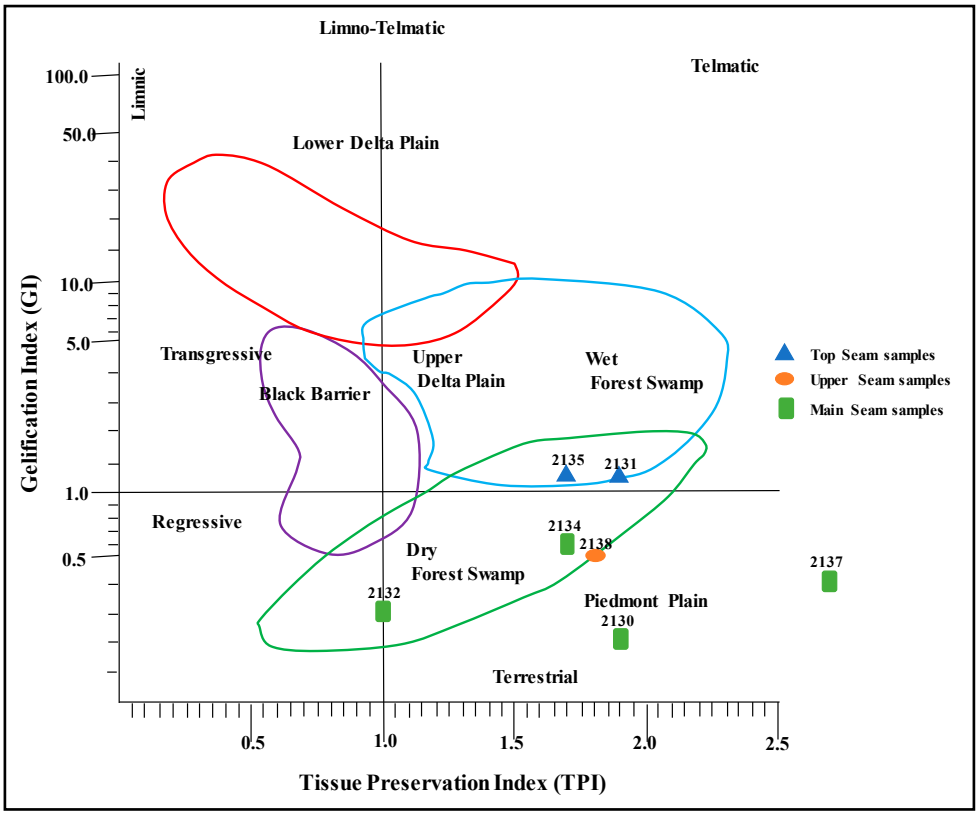

Figure 9. TPI/GI coal facies diagram for the Imaloto coals (modified from [43]).

The sedimentological footprints gathered from the stratigraphic column (Figure 2), together with the facies analyses above, demonstrate that the Coal Measures are part of a delta to coastal plain environment. In addition to coal seams, some of the most important indicators include wave and current ripple marks, thick fine-to-medium-grained sandstones interbedded with layers of siltstones with planar and tabular cross-stratification. The thickness of the delta/plain setting, which constitutes the Coal Measures, varies from 20 to 160 m, and the sandstone bodies in the distributary channels within these intervals are rather thick, possessing an upward-finning tendency and lower acute erosive concave margins. Coal seams and layers of siliciclastic carbonaceous shales occur at the foot of small coarsening upward cycles of sandstones, which indicates sea level transgression on the lower coal-bearing successions. The presence of wave ripple marks indicates marine influence on this part of the basin [46]. The coal seams typically have sharp contacts at the top and gradational contacts at the base. The sharp contacts above the coal seams indicate removal of a part of the peat precursor due to switching fluvial channels. Gradational contacts below coal seams indicate a continuity of deposition and genetic relationship between the siliciclastic sedimentary and coal facies [46].

6. Conclusions

Following the characterization of the petrography, geochemistry, and mineralogy of a fairly limited number of samples obtained from the Sakoa Group Coal Measures occurring in the Imaloto Basin, a sub-basin of the Morondava Basin of southwestern Madagascar, the following conclusions can be drawn.

- The Main Seam, which is at the bottom of the stratigraphic sequence in the Imaloto Basin, hosts the best quality coal in terms of CV, ash, and FC yield.
- In all three seams, better quality coals occur in the deeper central axial portions of the basin.

- Inertinite macerals are abundant in the Main Seam, while the Upper Seam and the Top Seam are vitrinite-rich.
- The vitrinite reflectance data indicate that these samples span between Sub-Bituminous Low Rank A and Medium Rank D.
- The abundance of the mineral analcime (or analcite) ($NaAlSi_2O_6 \cdot H_2O$) in samples occurring in all seams is of interest. Further studies may be required to confirm the identification of this mineral and to determine the source.
- The different qualities determined in these Imaloto coals are a reflection of the heterogenous nature of coal, which is related to the depositional environments. The failed rifting event that created the Morondava Basin, resulting in extensive extensional faulting, influenced the accumulation of vegetation and subsequent coalification and coal quality. It is evident from the petrographic data that the geological setting of the basin influenced the depositional environments, with the various coal seams forming in different paleoenvironments.
- It is suggested that further coal samples are obtained to confirm these initial findings and expand on the understanding of the coals occurring in the Imaloto Basin.

Author Contributions: M.B.N. PhD candidate at UJ. Developed the research project, obtained the samples, conducted the research, and wrote the manuscript. N.J.W. Supervisor. Guided the research, assisted with the petrography, and reviewed drafts of the manuscript. R.V. Co-Supervisor. Assisted with sample acquisition, developed the project, and reviewed drafts of the manuscript. All authors have read and agreed to the published version of the manuscript.

Funding: This work was in part supported by the Department of Science and Innovation (DSI)—National Research Foundation (NRF) Centre of Excellence for Integrated Mineral and Energy Resource Analysis (CIMERA; https://cimera.co.za/) (accessed on 30 May 2024), grant number 91487, and Lemur Holdings Ltd., as well as the authors.

Data Availability Statement: All data and information pertaining to this research are kept in a locked file on a private computer accessible only to the researchers. Data can be made available to readers upon request.

Acknowledgments: The project was supported by DSI-NRF CIMERA at the University of Johannesburg, and Lemur Holdings Ltd. Biswas, of the Department of Geology at UJ, is acknowledged for running the SEM-EDX analyses. This work forms part of a PhD in preparation by the first author.

Conflicts of Interest: The authors declare no conflicts of interest. The funders had no role in the design of the study; in the collection, analyses, or interpretation of data; in the writing of the manuscript; or in the decision to publish the results. The authors declare that they have no known competing financial interests or personal relationships that could have appeared to influence the work reported in this paper.

References

1. Worldometer. Population of Madagascar (Live). Available online: https://www.worldometers.info/world-population/madagascar-population/ (accessed on 18 September 2022).
2. World Bank. *Economic Contributions from Industrial Mining in Madagascar*; Research Summary; World Bank: Antananarivo, Madagascar, 2015; pp. 41–241.
3. World Bank. Madagascar: $150 Million to Increase Access to Electricity Services for Households, Enterprises, and Health Facilities. 2019. Available online: https://www.worldbank.org/en/country/madagascar (accessed on 30 May 2024).
4. Giese, J.; Seward, D.; Schreurs, G. Low temperature evolution of the Morondava rift shoulder in western Madagascar. In *Geophysical Research Abstracts, Proceedings of the EGU General Assembly 2010, Vienna, Austria, 2–7 May 2010*; European Geosciences Union (EGU): Vienna, Austria, 2012; Volume 12, p. EGU2010-11340.
5. Besairie, H. Géologie de Madagascar. Les terrains sédimentaires. In *Annales Géologiques de Madagascar*; Imprimerie Nationale: Tananarive, Madagascar, 1972; Volume 35, 552p.
6. Rabinowitz, P.D.; Coffin, M.F.; Falvey, D. The separation of Madagascar and Africa. *Science* **1983**, *220*, 67–69. [CrossRef] [PubMed]
7. Coffin, M.F.; Rabinowitz, P.D. *Evolution of the Conjugate East African-Madagascan Margins and the Western Somali Basin*; GSA Special Papers; Geological Society of America: McLean, VA, USA, 1988; Volume 226, 78p.
8. Clark, D.N. Review of the exploration potential of Madagascar. *Houst. Geol. Soc. Bull.* **1998**, *40*, 23–29.

9. Schandelmeier, H.; Bremer, F.; Holl, H. Kinematic evolution of the Morondava rift basin of SW Madagascar—From wrench tectonics to normal extension. *J. Afr. Earth Sci.* **2003**, *38*, 321–330. [CrossRef]
10. Cairncross, B. An overview of the Permian (Karoo) coal deposits of southern Africa. *Afr. Earth Sci.* **2001**, *33*, 529–652. [CrossRef]
11. Falcon, R.; Ham, A.J. The characteristics of Southern African coals. *J. S. Afr. Inst. Min. Metall.* **1988**, *88*, 145–161.
12. Hancox, P.J. The Coalfields of South-Central Africa: A Current Perspective. *Epis. J. Int. Geosci.* **2016**, *39*, 407–428. [CrossRef]
13. Ashwal, L.D.; Tucker, R.D. Geology of Madagascar: A brief outline. *Gondwana Res.* **1999**, *2*, 335–339. [CrossRef]
14. Piqué, A.; Laville, E.; Bignot, G.; Rabarimanana, M.; Thouin, C. L'ouverture et le développement du BasinMorondava (Madagascar) du Carbonifère supérieur au Jurassique moyen. Données stratigraphiques, sédimentaires, paléontoloqtques at structurales. *J. Afr. Earth Sci.* **1999**, *28*, 931–948. [CrossRef]
15. Nichols, G.J.; Daly, M.C. Sedimentation in an intra-cratonic extensional Basin: The Karoo of the central Morondava Basin, Madagascar. *Geol. Mag.* **1989**, *126*, 339–354. [CrossRef]
16. Langford, R.P. *Permian Coal and Palaeogeography of Gondwana*; Bureau of Mineral Resources, Geology and Geophysics: Canberra, Australian, 1992; 130p.
17. Wescott, W.A.; Diggens, J.N. Depositional history and stratigraphical evolution of the Sakoa Group (lower Karoo Supergroup) in the southern Morondava Basin Madagascar. *J. Afr. Earth Sci.* **1999**, *24*, 585–601. [CrossRef]
18. *SABS/ISO 7404-2*; Methods for the Petrographic Analysis of Coals Part 2: Methods of Preparing Coal Samples. International Organization for Standardization (ISO): Geneva, Switzerland, 2016.
19. *SABS/ISO 7404-3*; Methods for the Petrographic Analysis of Coals—Part 3: Method of Determining Maceral Group. International Organization for Standardization (ISO): Geneva, Switzerland, 2016.
20. *SABS/ISO 7404-5*; Methods for the Petrographic Analysis of Coals—Part 5: Method of Determining Microscopically the Reflectance of Vitrinite. International Organization for Standardization (ISO): Geneva, Switzerland, 2016.
21. Economic Commission for Europe Committee on Sustainable Energy (UN-ECE). *International Classification of In-Seam Coals*; United Nations: New York, NY, USA; Geneva, Switzerland, 1988.
22. *ISO/FDIS 11760*; Classification of Coals. International Organization for Standardization (ISO): Geneva, Switzerland, 2018.
23. Wadley, R.; Hall, M. Imaloto Coal Project: South-West Madagascar, Competent Person's Report and Resource Statement, MSA Project Number J2065, Johannesburg, South Africa. Unpublished report, 2010; pp. 5–25.
24. Badger Mining and Consulting, Johannesburg, South Africa. Imaloto Scoping Report. Unpublished Inhouse report. 2013.
25. Hagelskamp, H.B.; Snyman, C.P. On the origin of low-reflecting inertinites in coals from the Highveld Coalfield, South Africa. *Fuel* **1988**, *67*, 307–313. [CrossRef]
26. Hower, J.C.; Wagner, N.J.; O'Keefe, J.M.K.; Drew, J.W.; Stucker, J.D.; Richardson, A.R. Maceral types in some Permian Southern African coals. *Int. J. Coal Geol.* **2012**, *100*, 93–107. [CrossRef]
27. Semkiwa, P.; Kalkreuth, W.; Utting, J.; Mpanju, F.; Hagemann, H. The geology, petrology, palynology, and geochemistry of Permian coal basins in Tanzania. Songwe-Kiwira Coalfield. *Int. J. Coal Geol.* **2003**, *55*, 157–186. [CrossRef]
28. Maranha, S.; Machado, J.; Nascimento, L.; Peddollam, P.; Scholes, O. Mozambique Coal—The Uncommon Petrographic Quality and Its Consequences on the Coke Strength. 2013. Available online: http://www.repositorio.ufc.br/handle/riufc/57957 (accessed on 17 September 2022).
29. Taylor, G.H.; Teichnüller, M.; Davis, A.; Diessel, C.F.K.; Littke, R.; Robert, P. *Organic Petrology*; Gebrüder Borntraeger: Berlin, Germany, 1988; 704p.
30. Wagner, N.J.; Nandi, M.; Rosemary, M.S.F. *Southern African Coals and Carbons—Definitions and Applications of Organic Petrology*; Struik Nature: Cape Town, South Africa, 2018; 248p.
31. Falcon, R.M.S. A brief overview of the origin, formation and distribution of coal in southern Africa. In *Mineral Deposits of Southern Africa*; Anhaeusser, C.R., Maske, S., Eds.; Geological Society of South Africa: Johannesburg, South Africa, 1986; Volume 2, pp. 1879–1898.
32. Garcia-Vallès, M.; Pradell, T.; Martinez, S.; Vendrell, M. Mineralogical characterization of the Garumnian subbituminous lignite from the central Pyrenees by SEM-EDX, X-ray diffraction and Mössbauer spectroscopy. *Fuel* **1993**, *72*, 971–975. [CrossRef]
33. Roberts, D.L. The inherent moisture content of South African Permian coals. *Int. J. Coal Geol.* **1991**, *17*, 297–311. [CrossRef]
34. Dai, S.; Wang, X.; Zhou, Y.; Hower, J.C.; Li, D.; Chen, W.; Zhu, X.; Zou, J. Chemical and mineralogical compositions of silicic, mafic, and alkali tonsteins in the late Permian coals from the Songzao Coalfield, Chongqing, Southwest China. *Chem. Geol.* **2011**, *282*, 29–44. [CrossRef]
35. Pinheiro, H.J. (Ed.) *A Techno-Economic and Historical Review of the South African Coal Industry in the 19th and 20th Centuries, and Analysis of Coal Product Samples of South African Collieries 1998–1999*; Bulletin 113; SABS Coal Exploration and Technology: Pretoria, South Africa, 1999; 97p.
36. Christy, A.G. Australian New Minerals: 2008–Present. SGGMP Newsletter, 6–8 June 2010. Specialist Group for Geochemistry, Mineralogy and Petrology, Geological Society of Australia. Available online: https://physics.anu.edu.au/contact/people/download_publist.php?PeopleID=892 (accessed on 10 June 2024).
37. Dai, S.; Hower, J.C.; Finkelman, R.B.; Graham, I.T.; French, D.; Ward, C.R.; Eskenazy, G.; Wei, Q.; Zhao, L. Organic associations of non-mineral elements in Coal: A review. *Int. J. Coal Geol.* **2020**, *218*, 103347. [CrossRef]

38. Smyth, M. Coal microlithotypes related to sedimentary environments in the Cooper Basin, Australia. In *Sedimentology of Coal and Coal-Bearing Sequences*; Special Publication of the International Association of Sedimentologists; John Wiley & Sons: Hoboken, NJ, USA, 1984; Volume 7, pp. 333–347.
39. Mangs, A.D.; Wagner, N.J.; Moroeng, O.M.; Lar, U.A. Petrographic composition of coal within the Benue Trough, Nigeria and a consideration of the paleodepositional setting. *Int. J. Coal Sci. Technol.* **2022**, *9*, 35. [CrossRef]
40. Teichmüller, M. The genesis of coal from the viewpoint of coal petrology. *Int. J. Coal Geol.* **1989**, *12*, 1–87. [CrossRef]
41. International Committee for Coal and Organic Petrology (ICCP). The new inertinite classification (ICCP System 1994). *Fuel* **1994**, *82*, 459–471.
42. Suárez-Ruiz, I.; Crelling, J.C. (Eds.) *Applied Coal Petrology*; Elsevier: Amsterdam, The Netherlands, 2008; 388p.
43. Diessel, C.F.K. On the correlation between coal facies and depositional environments. In *Advances in the Study of the Sydney Basin Proceedings of the 20th Symposium of Department Geology*; University of Newcastel: Newcastle, NSW, Australia, 1986; pp. 19–22.
44. Calder, J.; Gibling, M.; Mukhopadhyay, P. *Peat Formation in a Westphalian B Piedmont Setting, Cumberland Basin, Nova Scotia: Implications for the Maceral-Based Interpretation of Rheotrophic and Raised Paleomire*; Contribution Series No. 91-002; Chamber of Mineral Resources of Nova Scotia: Halifax, NS, Canada, 1991.
45. Dai, S.; Bechtel, A.; Eble, C.F.; Flores, R.M.; Frend, D.; Graham, I.T.; Hood, M.M.; Hower, J.C.; Korasidis, V.A.; Moore, T.A.; et al. Recognition of peat depositional environments in coal: A review. *Int. J. Coal Geol.* **2020**, *219*, 103383.
46. Miall, A.D. *Principals of Sedimentary Basin Analysis*, 3rd ed.; Springer: Berlin/Heidelberg, Germany, 2000; p. 637.

Disclaimer/Publisher's Note: The statements, opinions and data contained in all publications are solely those of the individual author(s) and contributor(s) and not of MDPI and/or the editor(s). MDPI and/or the editor(s) disclaim responsibility for any injury to people or property resulting from any ideas, methods, instructions or products referred to in the content.